

# Scan-Statistic Approach Identifies Clusters of Rare Disease Variants in *LRP2*, a Gene Linked and Associated with Autism Spectrum Disorders, in Three Datasets

Iuliana Ionita-Laza,<sup>1,\*</sup> Vlad Makarov,<sup>2</sup> the ARRA Autism Sequencing Consortium,<sup>3</sup> and Joseph D. Buxbaum<sup>2,4,5,\*</sup>

Cluster-detection approaches, commonly used in epidemiology and astronomy, can be applied in the context of genetic sequence data for the identification of genetic regions significantly enriched with rare disease-risk variants (DRVs). Unlike existing association tests for sequence data, the goal of cluster-detection methods is to localize significant disease mutation clusters within a gene or region of interest. Here, we focus on a chromosome 2q replicated linkage region that is associated with autism spectrum disorder (ASD) and that has been sequenced in three independent datasets. We found that variants in one gene, *LRP2*, residing on 2q are associated with ASD in two datasets (the combined variable-threshold-test  $p$  value is  $1.2 \times 10^{-5}$ ). Using a cluster-detection method, we show that in the discovery and replication datasets, variants associated with ASD cluster preponderantly in 25 kb windows (adjusted  $p$  values are  $p_1 = 0.003$  and  $p_2 = 0.002$ ), and the two windows are highly overlapping. Furthermore, for the third dataset, a 25 kb region similar to those in the other two datasets shows significant evidence of enrichment of rare DRVs. The region implicated by all three studies is involved in ligand binding, suggesting that subtle alterations in either *LRP2* expression or *LRP2* primary sequence modulate the uptake of *LRP2* ligands. *BMP4* is a ligand of particular interest given its role in forebrain development, and modest changes in *BMP4* binding, which binds to *LRP2* near the mutation cluster, might subtly affect development and could lead to autism-associated phenotypes.

## Introduction

Advances in next-generation-sequencing technologies<sup>1</sup> facilitate large-scale sequencing studies and allow for a comprehensive investigation of the role that rare variants might play in complex diseases with the hope that rare variants can provide further insight into the underlying biology of these diseases. Ongoing sequencing studies are already generating unprecedented amounts of genetic data. The large number of genetic variants, most of which have low population frequencies, being uncovered in these datasets creates particular challenges for the statistical analysis of this new type of data. Already, many association tests for sequence data have been proposed.<sup>2–13</sup> These methods are concerned with rejecting the null hypothesis that variants in a gene or region are not associated with disease.

The focus in this paper is on the localization of rare disease-risk variants (DRVs) in a larger genetic region via a cluster-detection method. Unlike existing association tests that test for disease association with variants in a contained genetic region, the goal here is to find the window (within the larger region) in which DRVs cluster more significantly than they do in the rest of the region, i.e., outside of the window. Here, we describe a method that is specifically designed to identify such small regions enriched with DRVs and that is quite different from existing association tests (more details on the differences between cluster-detection methods and association tests will be

given later in the [Material and Methods](#) section). Cluster-detection methods are commonly used in applied sciences, such as in epidemiology for the identification of hotspots of disease cases (i.e., epidemics), as well as in astronomy for the identification of star clusters and galaxies. One popular class of methods is based on the use of scan statistics.<sup>14</sup> The underlying idea of scan-statistic methodology is to slide a window of fixed size  $w$  along the length of the region and compute an overall statistic for all windows of length  $w$ . We propose here a likelihood ratio (LR) statistic that takes into account the underlying spatial distribution of variants in the population; this LR statistic is similar to an approach proposed by Kulldorff.<sup>15</sup> For each window  $W$  of size  $w$ , we calculate the LR statistic,  $LR_W$ . The window  $W$  with the highest value for the  $LR_W$  is the most likely region to harbor a cluster of DRVs, and an approximate  $p$  value for the window with the largest  $LR_W$  is calculated by Monte Carlo simulations.

Clustering of disease mutations in small regions of a gene has been reported before for some Mendelian diseases and, more recently, for several complex traits as well. For example, highly localized mutations in the gene encoding the cytoskeletal protein filamin A (*FLNA* [MIM 300017]) lead to a broad range of congenital malformations in humans.<sup>16</sup> Similarly for Duchenne muscular dystrophy (MIM 310200) and the milder form, Becker muscular dystrophy (MIM 300376), mutations cluster in actin binding domain 1 (ABD1) of dystrophin<sup>17</sup> (MIM 300377). Other examples include Rett syndrome<sup>18</sup> (MIM 312750),

<sup>1</sup>Department of Biostatistics, Columbia University, New York, NY 10032, USA; <sup>2</sup>Seaver Autism Center for Research and Treatment, Mount Sinai School of Medicine, New York, NY 10029, USA; <sup>3</sup>ARRA Autism Sequencing Consortium membership is listed in the Acknowledgments; <sup>4</sup>Department of Psychiatry, Mount Sinai School of Medicine, New York, NY 10029, USA; <sup>5</sup>Genetics and Genomic Sciences, Mount Sinai School of Medicine, New York, NY 10029, USA

\*Correspondence: [ii2135@columbia.edu](mailto:ii2135@columbia.edu) (I.I.-L.), [joseph.buxbaum@mssm.edu](mailto:joseph.buxbaum@mssm.edu) (J.D.B.)

DOI 10.1016/j.ajhg.2012.04.010. ©2012 by The American Society of Human Genetics. All rights reserved.

hereditary angioneurotic edema<sup>19</sup> (MIM 106100), Von Willebrand disease type 2A<sup>20</sup> (MIM 613554), etc. For complex traits, not many of such studies have been published to date. A recent study focusing on somatic cancer mutations found that disease-causing mutations cluster more often than random mutations, suggesting that mutation hotspots occur at the domain level.<sup>21</sup> Similarly, a study on schizophrenia (MIM 181500) and bipolar disorder (MIM 125480) identified significant clustering of nonsynonymous SNPs in two exons encoding the cysteine-rich domain and first transmembrane helix of metabotropic (GRM1) glutamate receptor.<sup>22</sup> Here, we report for three independent datasets a clustering of rare DRVs in a small region of *LRP2* (MIM 600073), a gene residing in a replicated linkage region for autism spectrum disorder (ASD [MIM 209850]) on chromosome 2q.<sup>23–25</sup>

Autism and ASD are associated with high heritability. There have been successes in identifying chromosomal abnormalities and copy-number variants that contribute

## Scan Statistic for the Identification of Clusters of Rare DRVs

Let us assume that  $N$  unrelated individuals, both affected and unaffected, have been sequenced in a region or gene of interest  $G$ . Furthermore, let us assume that there are  $M$  rare-variant positions in the region of interest. A rare variant is identified as a variant with a minor allele frequency (MAF) that is less than a fixed threshold (e.g., 0.01) in controls. At each position  $i$  with  $i \leq M$ , let  $n_i$  be the number of individuals that carry a rare variant and let  $y_i$  be those that are affected. Therefore,  $y_i$  is binomial  $(n_i, p_i)$ , where  $p_i$  is related to the relative risk at position  $i$ . We are working under the assumption that there is a window  $W_{\text{dis}}$  such that  $p_i = p_{W_{\text{dis}}}$  for  $i \in W_{\text{dis}}$  and  $p_i = p_0$  for  $i \notin W_{\text{dis}}$ . Under the null hypothesis,  $p_{W_{\text{dis}}} = p_0$ , whereas the alternative hypothesis is that  $p_{W_{\text{dis}}} > p_0$ . For a fixed window size, we employ a sliding-window approach and calculate a LR statistic.

### Bernoulli Model

To calculate the LR statistic, we first condition on the window  $W$  and calculate for each window  $W$  of fixed size  $w$  the following LR score:

$$LR_W = \begin{cases} \left(\frac{\widehat{p}_W}{\widehat{r}_G}\right)^{y_W} \left(\frac{1-\widehat{p}_W}{1-\widehat{r}_G}\right)^{n_W-y_W} \left(\frac{\widehat{q}_W}{\widehat{r}_G}\right)^{y_G-y_W} \left(\frac{1-\widehat{q}_W}{1-\widehat{r}_G}\right)^{n_G-n_W-(y_G-y_W)} & \text{if } \widehat{p}_W > \widehat{q}_W, \\ 1 & \text{otherwise} \end{cases}$$

significantly to risk. These variants are individually rare but in combination are etiological factors in as much as 15% of ASD. Candidate-gene sequencing studies have identified many genes associated with high risk, and, with the advent of whole-exome and whole-genome sequencing, it is becoming possible to exhaustively explore the influence of rare variants, both single point and structural, on the risk of developing ASD.

We apply such a cluster-detection method to three independent ASD datasets. We identify *LRP2* in an ASD-linked region on chromosome 2q as being associated with ASD in two of the datasets. Furthermore, we show that rare risk variants cluster significantly in affected individuals in highly overlapping regions for all three datasets.

## Material and Methods

The underlying idea of scan-statistic methodology is to slide a window of fixed size  $w$  along the length of the region and compute a statistic  $S_w$ . For example, when testing whether points on a line are uniformly distributed,  $S_w$  could be the maximum number of points along the line in any window of size  $w$ . Wallenstein and Neff<sup>26</sup> derived the approximate distribution for  $S_w$  under the simplified assumption that points are independent and uniformly distributed across a region. However, it is well known that genetic-variant positions can cluster in a nonuniform fashion on the basis of purely biological reasons, and such a clustering might not be related to disease. Therefore, any reasonable method needs to take into account the underlying spatial distribution of variants in the population. Kulldorff<sup>15</sup> described a LR statistic, and we follow a similar approach here.

where

$$\begin{aligned} y_W &= \sum_{i \in W} y_i \text{ and } y_G = \sum_{i \in G} y_i, \\ n_W &= \sum_{i \in W} n_i \text{ and } n_G = \sum_{i \in G} n_i, \\ \widehat{p}_W &= \frac{y_W}{n_W} \text{ and } \widehat{q}_W = \frac{y_G - y_W}{n_G - n_W}, \\ \text{and } \widehat{r}_G &= \frac{y_G}{n_G}. \end{aligned}$$

Note that  $\widehat{p}_W$  and  $\widehat{q}_W$  are the maximum likelihood estimators (MLEs) under the alternative hypothesis, whereas  $\widehat{r}_G$  is the MLE under the null hypothesis. A pseudocount of 1 is added when the proportions  $p_W$ ,  $q_W$ , and  $r_G$  are estimated.

The LR statistic for window size  $w$  is then computed as

$$\Lambda_w = \max_{|W|=w} LR_W.$$

The window  $W$  with the highest value for the  $LR_W$  is the most likely region to harbor a cluster of DRVs.

### Definition of Windows $W$

The definition of the windows  $W$  for consideration is flexible and depends on the region under investigation, such as its length. The unbiased, agnostic approach is to consider all contiguous (and overlapping) windows of a fixed size  $w$ . Another possibility is to define windows on the basis of known biological features, such as known functional domains. This could be more powerful than the agnostic approach because it might lead to increased signal in the windows being tested and also reduced penalty for multiple-testing correction.

In the agnostic approach, the size of the sliding window,  $w$ , is not known a priori; therefore, we can consider several distinct

window sizes and evaluate the overall significance by permutation. More precisely, we can define the generalized LR statistic as the following:

$$GLR = \max_w \max_{|W|=w} LR_W.$$

We call this the variable window (VW) approach because multiple window sizes are considered. The maximum window size considered is, at most, 50% of the total region length.

### Statistical Significance

For the purposes of inference, we compute the above  $LR_W$  statistics for all windows  $W$  that we choose to consider. Let  $\Lambda_w = \max_W LR_W$ .

Standard asymptotic-theory results do not apply<sup>1</sup> here (1) because of the implicit assumption of independence among different rare variants in the likelihood calculation and (2) because the parameter  $W_{dis}$  disappears under the null hypothesis and is only present under the alternative.<sup>27</sup> Therefore, we use Monte Carlo simulations to compute the  $p$  value for  $\Lambda_w$ . We permute the affection-status labels and then recalculate the maximum LR statistic across all windows as was done for the original study. A similar permutation procedure is performed for the VW approach, which maximizes over multiple window sizes. Note that the resulting  $p$  values are adjusted for multiple testing (i.e., for all overlapping windows that are being considered).

## Results

### Simulated Data

#### Type-1 Error and Power

We use simulations to investigate the underlying properties of the proposed approaches. We simulated one 1 Mb genomic region under a coalescent model by using the software package COSI.<sup>28</sup> The model used in the simulation was the calibrated model for the European population and was an option available in the COSI package (the best-fit model). A total of 10,000 haplotypes were generated. We then randomly sampled small regions of the size of individual genes (between 1.5 and 200 kb).

To evaluate the type-1 error, we derived datasets of 300 cases and 300 controls under the null hypothesis of no association between any of the variants and disease.

To evaluate the power of the approach, we assume that a subregion is enriched with rare DRVs. The percentage of DRVs in a simulated gene is assumed to be 20% for genes of length 10 kb and 20 kb and 3%–10% for larger genes (i.e., 50–200 kb). We have also considered smaller genes of sizes 1.5 kb and 3 kb and assumed that 20%–50% of variants are DRVs. DRVs are chosen to be variants that have a frequency less than 0.01 and that reside in a small subregion of the gene. Assuming  $D$  DRVs, then dichotomous phenotypes are simulated from

$$\text{logit } P(y = 1) = \beta_0 + \sum_{j=1}^D \beta_j X_j,$$

where  $\beta_0 = \text{logit}(0.05)$ . We can specify the effect size at each DRV by setting  $\beta_j = c|\log_{10}(MAF_j)|$  for the  $j^{\text{th}}$  disease variant. We take  $c = 0.549$ , which results in an odds ratio (OR) of 9 for variants with  $MAF = 10^{-4}$  and an OR of 5.2

**Table 1. Simulated Data**

$\alpha$	Type-1 Error Rates			
	$w = 2 \text{ kb}$	$w = 5 \text{ kb}$	$w = 8 \text{ kb}$	VW
0.05	0.049	0.061	0.055	0.055
0.01	0.008	0.012	0.014	0.012

Reported in the table are empirical type-1 error rates corresponding to nominal  $\alpha$  levels of 0.05 and 0.01. The size,  $w$ , of the sliding window can take three possible values between 2 and 8 kb. There are 300 cases and 300 controls. The variable window (VW) approach corresponds to maximizing over windows of length between 2 and 8 kb.

for variants with  $MAF = 10^{-3}$ . For a large 200 kb gene, we take  $c = 0.400$ , which results in an OR of 4.9 for variants with  $MAF = 10^{-4}$  and an OR of 3.3 for variants with  $MAF = 10^{-3}$ .

**Type-1 Error.** In Table 1, we report the empirical type-1 error for the clustering approach described above when it is applied to data simulated under the null hypothesis of no association between any of the variants in the region and disease. Different window sizes are considered between 2 and 8 kb. As shown, the empirical type-1 error agrees well with the nominal one.

**Power.** In Table 2, we report power estimates by using simulated data. Power is averaged over randomly chosen regions with lengths between 10 and 20 kb. Similar results are shown in Table A1 for regions of larger size, i.e., 50–200 kb.

The power of the cluster-detection approach depends critically on the length of the cluster window. As shown in Table 2, the power decreases when the size of the cluster window increases relative to the entire region. This is expected because the larger the size of the cluster, the weaker the evidence that DRVs cluster in any particular small region. The size of the scanning window is also important, and the power can vary dramatically depending on that. In particular, the power decreases substantially when the scanning window is too large. Intuitively, the optimal size is the cluster's true size, which is unknown to us. Therefore, we have proposed maximizing over multiple window sizes (the VW approach), an approach which compares well to the optimal power, as we show in simulations (Tables 2, A1, and A3).

**Table 2. Simulated Data**

Gene Length (kb)	Cluster Length (kb)	% DRVs	Power			
			$w = 2 \text{ kb}$	$w = 5 \text{ kb}$	$w = 8 \text{ kb}$	VW
10	2.4	20%	0.77	0.59	0.28	0.73
10	4.8	20%	0.37	0.47	0.31	0.49
20	4.8	20%	0.84	0.96	0.85	0.95
20	9.5	20%	0.52	0.70	0.80	0.64

Power is at  $\alpha = 0.05$ . There are 300 cases and 300 controls. Gene length refers to the length of the gene, and cluster length refers to the length of the cluster of DRVs. Power is averaged over randomly selected genes of fixed length. 20% of variants in a gene are assumed to be DRVs.

**Table 3. Simulated Data**

Gene Length (kb)	Cluster Length (kb)	% DRVs	Jaccard Index of Overlap			
			w = 2 kb	w = 5 kb	w = 8 kb	VW
10	2.4	20%	0.69	0.41	0.22	0.66
10	4.8	20%	0.35	0.74	0.49	0.60
20	4.8	20%	0.37	0.83	0.57	0.75
20	9.5	20%	0.19	0.47	0.72	0.54

Shown is the overlap between the true cluster region and the estimated cluster region as measured by the Jaccard index of overlap. There are 300 cases and 300 controls. Gene length refers to the length of the gene, and cluster length refers to the length of the cluster of DRVs. The index of overlap is averaged over randomly selected genes of fixed length. 20% of variants in a gene are assumed to be DRVs.

Power will generally be low for genes with little variation, as might be the case with small genes. We have looked at genes of sizes 1.5 kb and 3 kb and show that power can be quite low even if a large percentage (50%) of variants are in fact disease related (Table A3). In such cases, the clustering problem becomes less interesting because of the small number of observed variants in such small genes, and a simple gene-based association test will be more powerful.

#### Estimation of Cluster Location

Another important measure of performance for the proposed method is the overlap between the true simulated cluster region ( $T$ ) and the estimated cluster region ( $E$ ), namely the window with the maximum LR score. One natural measure of overlap between two regions  $T$  and  $E$  is the Jaccard index of overlap, defined as the size of the intersection divided by the size of the union of the two regions:

$$J(T, E) = \frac{|T \cap E|}{|T \cup E|}.$$

If the two regions are disjoint, then  $J(T, E) = 0$ , and if the two regions coincide, then  $J(T, E) = 1$ .

In Table 3, we report the overlap between the true and estimated cluster regions for the same scenarios for which power was reported in Table 2 (also see Tables A2 and A4). As with power, the highest overlap is achieved when the scanning-window size is close to the true cluster size. We also note that, as with power, the VW approach results in good overlap with the true region (values for the Jaccard index of overlap are over 0.50 in the simulated scenarios).

#### Clustering Versus Self-Contained Tests

Such a cluster-detection approach is ideal in situations in which multiple DRVs cluster in a small window of a gene. An alternative statistic for each window would be any of the sequence-based association statistics (e.g., burden statistics) already proposed in the literature comparing affected and unaffected individuals sequenced in a region of interest. The latter test is called a self-contained test in that, unlike the proposed procedure, it does not compare the association signal in a window with the association signal that is outside.

The two types of tests are designed for different goals. In particular, the null hypotheses for the two tests are

different. For the proposed test, the null hypothesis is that the DRVs are distributed as expected on the basis of the spatial distribution of variants in the population for that gene, whereas for the self-contained test, the null hypothesis is that there is no association between any of the variants in the gene and disease. If the latter is true, i.e., no association, then the former is true too, i.e., no clustering. The converse, however, is not true. It is possible that variants associated with disease do not cluster. It is only the proposed test that can identify significant clustering of rare DRVs, whereas the self-contained test can only identify significant association in a window, but that does not imply there is significant clustering of rare DRVs in that window.

Another important difference between the two methods is in the precision of estimation of cluster boundaries. We have compared the proposed clustering approach with two self-contained tests by using simulated data. We have simulated a gene of size 20 kb and assumed that 20% of all the variants in the gene are DRVs; 66% of DRVs cluster in a 3.5 kb window, whereas the rest are uniformly distributed. We then used a scanning window of size  $w = 4$  kb, and for each such window, we calculated three statistics: (1) the  $\log(\text{LR})$  statistic proposed here, (2) the  $Z$  score from the burden test, and (3) the  $p$  value from the collapsing method,<sup>2</sup> all of which are restricted to variants with  $\text{MAF} \leq 0.01$ . We show in Figure 1 that the clustering-based approach correctly identifies the true cluster window of size 3.5 kb, whereas the burden test and the collapsing test lead to noisier results (more results are shown in the Supplemental Data). Furthermore, it is not clear from the results of the burden or collapsing tests whether there is significant clustering or not; this is naturally so given that such self-contained tests are designed to test for association and not clustering.

## Application to ASD

### Discovery Dataset

For the discovery stage, we have used sequence data generated in Faham et al.<sup>29</sup> In that study, the authors sequenced (by using mismatch-repair detection on tag arrays) approximately 397 ASD patients and 450 controls; they mostly targeted coding regions of 68 genes within a 20 Mb chromosome 2q linkage peak that has been implicated in ASD by multiple whole-genome linkage scans.

First, we applied the variable threshold (VT) association test<sup>4</sup> and tested each of the 68 genes in the linked region on chromosome 2q. By using the VT method and maximizing over several MAF thresholds between 0.01 and 0.50, two genes, namely *LRP2* ( $p = 7.4 \times 10^{-5}$ ) and *CMYA3* ( $p = 10^{-5}$  [MIM 609778]) are region-wide significant (Figure 2). The  $p$  values for *LRP2* and *CMYA3* were calculated with several MAF thresholds (Table A5).

*LRP2* is a long gene (~235 kb), and we have performed a clustering analysis to investigate whether rare DRVs cluster preponderantly in a small window of the gene. We have calculated the LR statistic for all overlapping windows of lengths between 5 and 30 kb and have identified one

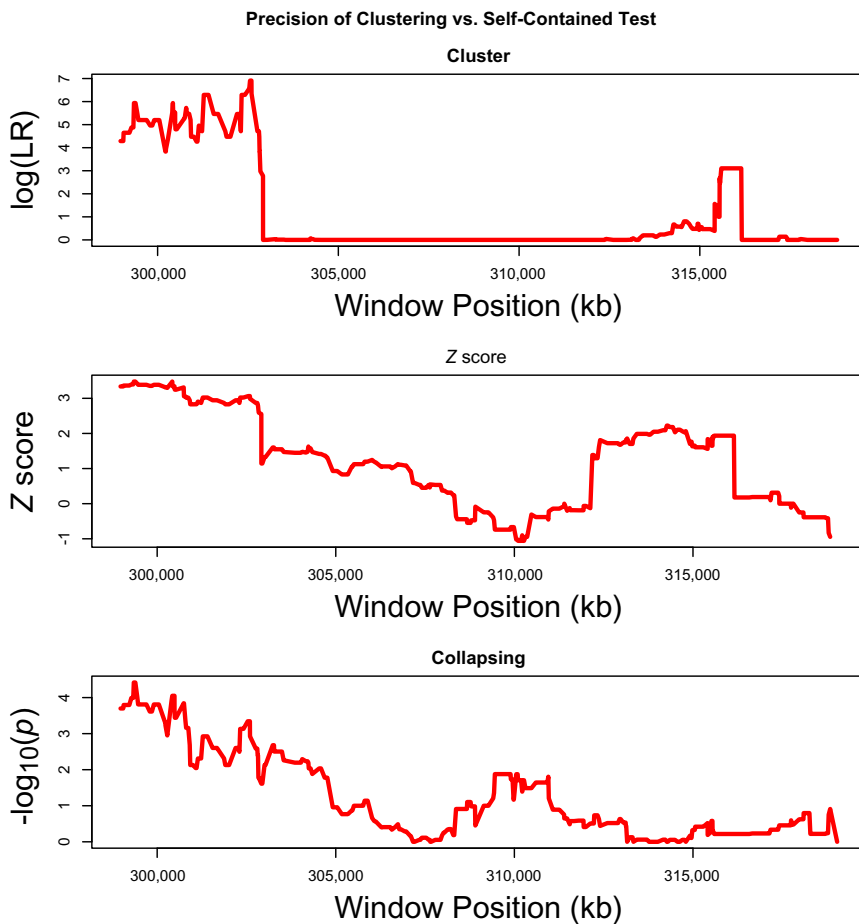


**Figure 1. Clustering Versus Self-Contained Tests**

Precision of estimation of the cluster boundaries for a simulated cluster region. A 20 kb gene is simulated with DRVs clustered in a 3.5 kb window at the start of the gene. From top to bottom, the graphs depict a cluster test, a burden test, and a collapsing test.

25 kb window (170,072,764–170,097,764; hg19) that is enriched with rare risk variants (the  $p$  value adjusted for all 25 kb windows is 0.003; Figure 3). The  $p$  values for other window sizes are shown in Table 4. The  $p$  value adjusted for testing all windows with lengths between 5 and 30 kb is 0.01. The variant amplicons in this window, together

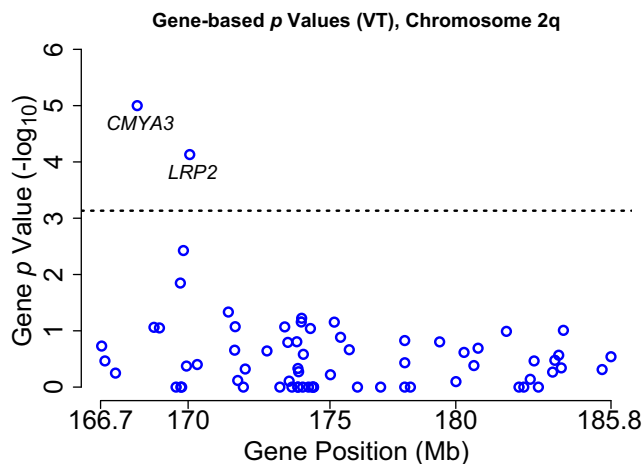


**Figure 2. Empirical  $p$  Values for 68 Genes Sequenced in the Linked Region on Chromosome 2q<sup>29</sup>**

Two genes, namely *LRP2* and *CMYA3*, remain significant after multiple-testing correction.

with observed frequency counts in cases and controls, are shown in Table A6. Note that for the clustering analysis, variant amplicons with a frequency less than 0.10 in controls were included in the analysis. With a frequency threshold of 0.01, the same peak region is identified, and the  $p$  value (adjusted for all windows with sizes between 5 and 30 kb) is 0.054, whereas for a frequency threshold of 0.05, the  $p$  value is 0.040.

*LRP2* is a member of the low density lipoprotein receptor (*LDLR* [MIM 606945]) gene family, and, like *LDLR*, *LRP2* can bind ApoE as well as a large variety of additional ligands. The expression of *LRP2* in the brain and the functional importance of some *LRP2* ligands have indicated that *LRP2* plays a role in neuronal develop-

ment and regeneration.<sup>30</sup> Recently, a de novo deleterious mutation in *LRP2* was found by whole-exome sequencing in one ASD case.<sup>31</sup> Defects in *LRP2* are known to cause Donnai-Barrow (aka, facio-oculo-acoustico-renal) syndrome,<sup>32</sup> a rare neurological disease. Furthermore, mutations in *LRP2* have been shown to disrupt cortical development in mice.<sup>33</sup> *LRP2* is also known to play a role in brain development,<sup>34</sup> including forebrain development, through its effects on sonic hedgehog (Shh) signaling.<sup>35</sup> Specifically, *LRP2* binds BMP4, leading to its internalization and catabolism, and reduced levels of *LRP2* are associated with elevated BMP4 and disruption of normal brain development.<sup>35,36</sup> Also, *LRP2* has been shown to be an auxiliary receptor for Sonic hedgehog by regulating the tracking of the SHH/PTCH1 complex.<sup>37</sup> Gene-dosage abnormalities at *PTCH1* lead to a syndrome that includes developmental delay and/or intellectual disability, as well as occasionally autism along with other features.<sup>38, 39, 40</sup> In van der Zwaag et al.<sup>41</sup> the authors used knowledge on functional gene networks to perform a topology-corrected Prioritizer analysis<sup>42</sup> and report the top ten genes out of 109 genes in the 2q linked region. *LRP2* ranks first among these 109 genes with a  $p$  value of 0.007.

The cluster window maps to a region that includes four tandem epidermal growth factor (EGF) precursor homology domains, particularly the two most NH-terminal

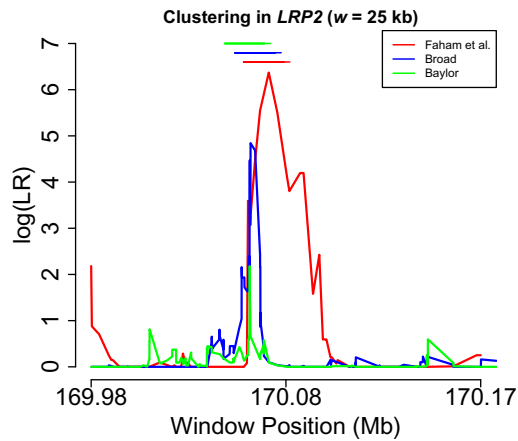


**Figure 3. Clustering of Rare DRVs in *LRP2* for Three Datasets**  
For each window, the midpoint is plotted on the  $x$  axis. The 25 kb windows with maximum LR score are also shown for the three datasets. Scanning-window length is  $w = 25$  kb.

domains. This is just downstream of the domain that binds RAP, and the fact that there is evidence that BMP4 and RAP share binding sites in *LRP2*<sup>35</sup> suggests that alterations in the interaction of *LRP2* with BMP4 caused by various mechanisms, including changes in protein levels or primary amino acid sequence, can lead to subtle changes in forebrain development, an area of great importance in autism-related phenotypes.

The original Faham et al.<sup>29</sup> study concentrated on more common variants and only reported the association with variants in *CMYA3*, although an independent replication attempt failed at that time. There are only 13 variants observed in this gene, which makes a clustering analysis for this gene not meaningful.

#### Replication Datasets

We have used an independent dataset to replicate the finding on the risk-variant cluster within *LRP2*. Hence, we have applied the cluster-detection approach to a second dataset (ARRA-Broad; see Appendix A for more information) consisting of 430 cases and 379 controls sequenced in the exonic regions of *LRP2*. We have identified a 25 kb window of significant clustering resulting in a  $p$  value (adjusted for all 25 kb windows) of 0.038, and the window with the maximum LR statistic is 170,068,479–170,093,479. If only nonsynonymous variants are considered, the adjusted  $p$  value for all 25 kb windows is 0.02 and the  $p$  value

adjusted for all overlapping windows with lengths between 5 and 30 kb is 0.01 (Table 4). The variants in this window, together with functional annotations and observed frequency counts in cases and controls, are shown in Table A7. Note that this window overlaps substantially with the window detected in the discovery dataset (i.e., 170,072,764–170,097,764; the Jaccard index of overlap is 0.71). In Figure 3, we plot for each window  $W$  of size 25 kb the corresponding  $\log(LR_W)$  values for the two datasets. There is substantial overlap between the windows of maximum LR score in the two datasets, although the signal is, as expected, stronger in the discovery dataset than in the replication dataset. Also, because of the smaller number of variants in the discovery dataset, the peak for the discovery dataset is also broader in that case.

If we perform an overall test of association at the gene level, variants in *LRP2* are significantly associated with ASD (VT-test  $p$  value of 0.011). The combined VT-test  $p$  value based on the two datasets is  $1.2 \times 10^{-5}$ . Restriction to only nonsynonymous variants did not result in significant results (probably as a result of the ensuing exclusion of common variants, some of which are associated with ASD as we show below). Also, there is no evidence of association in this dataset with variants in *CMYA3*.

**Common Variant Analysis in *LRP2*.** We have also tested for association between the common variants in *LRP2* ( $MAF \geq 0.05$ ) and ASD by using the software package PLINK. Of 32 variants with  $MAF \geq 0.05$ , ten of them have  $p$  values (Cochran-Armitage test) less than 0.05 (although they are not all independent signals), and all of them are in the same direction (Table A8). Compared with the unassociated variants, these associated variants are substantially closer to the enriched window above; all of the ten associated variants are within 10 kb of the 25 kb window identified above. In addition, we have performed a gene-based test in PLINK for the common variants, and the  $p$  value is 0.03.

**Second Replication Dataset.** We have used a second replication dataset (ARRA-Baylor; see Appendix A for more information) consisting of 502 cases and 489 controls. When the scanning window size  $w$  is 25 kb (as above), we find that the window of maximum LR score is 170,063,380–170,088,380, which again highly overlaps with the cluster windows in the previous two datasets (Figure 3). The  $p$  values for enrichment in this window compared with that in the rest of the gene are 0.015 (for

**Table 4. *LRP2* Results**

Dataset	$p$ Value					
	$w = 5$ kb	$w = 10$ kb	$w = 20$ kb	$w = 25$ kb	$w = 30$ kb	VW
Discovery	0.019	0.007	0.005	0.003	0.002	0.010
ARRA-Broad	0.134	0.070	0.035	0.038	0.200	0.099
ARRA-Broad-NS	0.151	0.080	0.011	0.002	0.008	0.010

Shown are  $p$  values for the LR statistic ( $\Lambda_w = \max_{|W|=w} LR_W$ ) when window size  $w$  is between 5 and 30 kb, and variants with  $MAF \leq 0.1$  (Discovery) and  $f \leq 0.01$  (ARRA-Broad) are considered. VW corresponds to the variable-window approach of maximizing over multiple window sizes between 5 and 30 kb. The following abbreviation is used: NS, nonsynonymous only.

all variants) and 0.010 (for nonsynonymous variants only). Although these  $p$  values are specific to that window and do not survive correction for multiple testing for all overlapping 25 kb windows (as was the case for the previous two datasets), the evidence of significant clustering in the same region adds to the evidence from the first two datasets. Results remain significant ( $p < 0.05$ ) if other window sizes (between 5 and 30 kb) are considered as well.

**Randomized Sampling.** To show more evidence that the observed cluster windows in the three datasets are likely to represent bona fide regions enriched with rare DRVs, we have performed simple randomization experiments. In one example, cases and controls were randomly mixed and the cluster-detection method was then applied to the resulting datasets. As shown in Figure A1, the results are consistent with the null model of no clustering. In particular, the windows in which the maximum LR score is achieved for the three datasets are all disjoint. Similar results hold when cases and controls are completely interchanged.

## Discussion

By using a scan-statistic approach, we have identified clusters of rare DRVs in *LRP2*, which resides in a replicated ASD linkage region within chromosomal region 2q31.1 and which we have also shown to be associated with ASD on the basis of two independent datasets. Our applications to three independent ASD datasets revealed three highly overlapping 25 kb *LRP2* regions that are more significantly enriched with rare DRVs than is the rest of the gene.

Such a cluster-detection approach is ideal in cases where multiple rare DRVs cluster in a small region of a gene. When the gene under consideration is large, as is the case with *LRP2*, replication of association signals at the gene level can be challenging, and identification of such overlapping cluster regions can be important evidence of replicable signal. Furthermore, identifying such a cluster of genetic risk factors, when it exists, is important because it might provide insights into the underlying biological mechanism for the disease. The cluster region identified in our studies is involved in ligand binding. One mechanism that is consistent with the results is that subtle alterations in either *LRP2* expression or *LRP2* primary sequence modulate the uptake of *LRP2* ligands. BMP4 is a ligand of particular interest given

its role in forebrain development. Disruption of *LRP2* has been shown to lead to excess levels of BMP4 and disrupted development of the prosencephalon. Even modest changes in BMP4 binding might subtly affect development and could lead to autism-associated phenotypes.

Some of the problems that affect association tests in general are also relevant for the cluster method discussed here. Like the burden tests of association, the proposed method assumes that the effects of variants are all in the same direction. In some cases, it is possible that a mixture of risk and protective variants is present in a region, especially if the region under consideration is large. Although it is probably less likely for this scenario to happen in a small cluster region that might correspond to a functional domain, when this happens, the power for identifying a cluster will decrease. Population stratification is also a potential concern for the proposed method. However, because the enrichment of rare disease variants in a window is contrasted with that outside of the window, the stratification would generate a clustering effect only if a small portion of the larger region were to be affected by population stratification.

The proposed cluster-detection method is designed specifically to identify small windows (within a larger region) that have significantly more rare DRVs than the rest of the region. As such, it is very different from existing association tests that test for association between variants in a contained genetic region and disease and which cannot, by definition, implicate clustering of rare disease variants in any part of the region under consideration. Therefore, the proposed method complements existing region-based association tests and can be useful in identifying the parts of a gene or region that are involved in disease etiology.

## Appendix A: Data Generation and Processing for the AASC Data

The replication datasets have been sequenced as part of the ARRA Autism Sequencing Collaboration. Whole-exome sequencing of the samples was carried out at the Broad Institute and at the Baylor College of Medicine via standard approaches.

Sequence-data processing and variant calling were performed with similar workflows at both sites. Data were processed with Picard<sup>43</sup> (see Web Resources) and BWA<sup>44</sup> for

**Table A1. Simulated Data for Large Genes**

Gene Length (kb)	Cluster Length (kb)	% DRVs	Power				VW
			w = 5 kb	w = 10 kb	w = 20 kb	w = 30 kb	
50	2.9	5%	0.92	0.68	0.35	–	0.95
50	6.0	10%	1.00	0.97	0.80	–	0.99
200	22	3%	0.66	–	0.68	0.63	0.63
200	25	5%	0.85	–	0.99	0.95	0.90

Power is at  $\alpha = 0.05$ . There are 300 cases and 300 controls. Gene length refers to the length of the gene, and cluster length refers to the length of the cluster of DRVs. Power is averaged over randomly selected genes of fixed length. 3% – 10% of variants in a gene are assumed to be DRVs. The following abbreviations are used: DRV, disease risk variant;  $w$ , window size; and VW, variable-window approach.

**Table A2. Simulated Data for Large Genes**

Gene Length (kb)	Cluster Length (kb)	% DRVs	Jaccard Index of Overlap				
			w = 5 kb	w = 10 kb	w = 20 kb	w = 30 kb	VW
50	2.9	5%	0.57	0.23	0.09	–	0.49
50	6.0	10%	0.69	0.55	0.28	–	0.68
200	22	3%	0.18	–	0.59	0.58	0.55
200	25	5%	0.17	–	0.72	0.63	0.72

Shown is the overlap between the true cluster region and the estimated cluster region as measured by the Jaccard index of overlap. There are 300 cases and 300 controls. Gene length refers to the length of the gene, and cluster length refers to the length of the cluster of DRVs. The index of overlap is averaged over randomly selected genes of fixed length. 3% – 10% of variants in a gene are assumed to be DRVs. The following abbreviations are used: DRV, disease risk variant; w, window size; and VW, variable-window approach.

**Table A3. Simulated Data for Small Genes**

Gene Length (kb)	Cluster Length (kb)	% DRVs	Power					
			w = 0.2 kb	w = 0.5 kb	w = 0.8 kb	w = 1.0 kb	w = 1.5 kb	VW
3.0	0.7	20%	–	0.22	–	0.42	0.25	0.46
3.0	1.7	50%	–	0.08	–	0.32	0.26	0.26
1.5	0.3	20%	0.28	0.30	0.20	–	–	0.14
1.5	0.8	50%	0.14	0.15	0.32	–	–	0.15

Power is at  $\alpha = 0.05$ . There are 300 cases and 300 controls. Gene length refers to the length of the gene, and cluster length refers to the length of the cluster of DRVs. Power is averaged over randomly selected genes of fixed length. 20% – 50% of variants in a gene are assumed to be DRVs. The following abbreviations are used: DRV, disease risk variant; w, window size; and VW, variable-window approach.

**Table A4. Simulated Data for Small Genes**

Gene Length (kb)	Cluster Length (kb)	% DRVs	Jaccard Index of Overlap					
			w = 0.2 kb	w = 0.5 kb	w = 0.8 kb	w = 1.0 kb	w = 1.5 kb	VW
3.0	0.7	20%	–	0.41	–	0.46	0.32	0.48
3.0	1.7	50%	–	0.25	–	0.44	0.61	0.55
1.5	0.3	20%	0.31	0.29	0.20	–	–	0.32
1.5	0.8	50%	0.20	0.47	0.49	–	–	0.37

Shown is the overlap between the true cluster region and the estimated cluster region as measured by the Jaccard index of overlap. There are 300 cases and 300 controls. Gene length refers to the length of the gene, and cluster length refers to the length of the cluster of DRVs. The index of overlap is averaged over randomly selected genes of fixed length. 20% – 50% of variants in a gene are assumed to be DRVs. The following abbreviations are used: DRV, disease risk variant; w, window size; and VW, variable-window approach.

**Table A5. Discovery Dataset**

Gene	p Value		
	MAF 0.01	MAF 0.10	VT
<i>LRP2</i>	$1.2 \times 10^{-2}$	$4.4 \times 10^{-4}$	$7.4 \times 10^{-5}$
<i>CMYA3</i>	$3.8 \times 10^{-1}$	$8.0 \times 10^{-2}$	$1.0 \times 10^{-5}$

*LRP2* and *CMYA3* p values calculated with minor allele frequency (MAF)  $\leq$  {0.01, 0.10} and with the variable threshold (VT) approach maximizing over multiple MAF thresholds.

**Table A6. *LRP2* Variants in the 25 kb Window of Maximum  $LR_w$  from the Discovery Dataset**

Position	Amplicon Length	Gene	$f_A$	$f_U$
170,072,764	259	<i>LRP2</i>	0.005	0.000
170,076,965	198	<i>LRP2</i>	0.006	0.000
170,081,821	219	<i>LRP2</i>	0.001	0.000
170,082,933	257	<i>LRP2</i>	0.009	0.007
170,088,225	199	<i>LRP2</i>	0.093	0.115
170,089,922	258	<i>LRP2</i>	0.020	0.006
170,094,602	274	<i>LRP2</i>	0.003	0.005
170,097,689	258	<i>LRP2</i>	0.026	0.011



**Table A7. LRP2 Variants in the 25 kb Window of Maximum  $LR_w$  from the ARRA Broad Study**

Position	ID	$f_A$	$f_U$	refAA	varAA	Function
170,068,479	–	0.0011	0	Gln	Gln	silent
170,068,502	rs146149181	0.0023	0	Thr	Ser	missense
170,068,598	rs138269726	0.0046	0	Asp	Asn	missense
170,068,628	rs142266106	0	0.0013	Ala	Thr	missense
170,068,709	–	0.0011	0	Glu	Lys	missense
170,068,710	rs144449508	0.0034	0.0013	Ala	Ala	silent
170,068,713	rs34834388	0.039	0.025	Ala	Ala	silent
170,070,172	rs4667596	0.017	0.022	Arg	Lys	missense
170,070,225	–	0.0011	0	Lys	Lys	silent
170,070,275	–	0.0011	0	Glu	Gln	missense
170,070,348	rs11886219	0.051	0.050	Arg	Arg	silent
170,070,365	rs41268689	0.0011	0	Val	Met	missense
170,072,797	–	0.0011	0	Gln	Arg	missense
170,077,014	–	0	0.0013	Thr	Thr	silent
170,082,013	rs2075246	0.43	0.38	–	–	–
170,082,936	rs138070797	0.0069	0.0013	Asn	Ser	missense
170,088,351	rs2302694	0.104	0.106	Ser	Ser	silent
170,089,934	rs145384264	0.020	0.011	Ser	Ser	silent
170,090,040	–	0.0011	0	Arg	His	missense
170,090,041	–	0.0011	0	Arg	Cys	missense
170,090,105	–	0	0.0013	–	–	–
170,090,139	rs78750385	0.0069	0.0065	–	–	–
170,092,386	–	0	0.0013	Asn	Lys	missense
170,092,395	rs2229267	0.26	0.21	Cys	Cys	silent
170,092,439	rs151079411	0.0023	0.0013	Leu	Leu	silent
170,092,467	rs141068435	0	0.0013	Cys	Cys	silent
170,092,504	–	0.0011	0	Arg	His	missense
170,092,613	rs74457112	0.0011	0	–	–	–

**Table A8.  $p$  Values from the Cochran-Armitage Trend Test for the Common LRP2 Variants Significantly<sup>a</sup> Associated with ASD**

Chr	Position	$f_A$	$f_U$	$p$ Trend	OR
2	170,103,351	0.49	0.41	0.0007	1.40
2	170,099,895	0.49	0.42	0.0037	1.33
2	170,099,473	0.48	0.41	0.0040	1.33
2	170,099,899	0.48	0.41	0.0044	1.33
2	170,099,446	0.48	0.41	0.0045	1.33
2	170,103,336	0.48	0.41	0.0045	1.33
2	170,092,395	0.26	0.21	0.0084	1.33
2	170,096,018	0.33	0.27	0.011	1.31
2	170,115,588	0.49	0.43	0.014	1.27
2	170,066,022	0.20	0.17	0.045	1.29

The following abbreviations are used: Chr, chromosome; and OR, odds ratio.

<sup>a</sup> $p < 0.05$ .

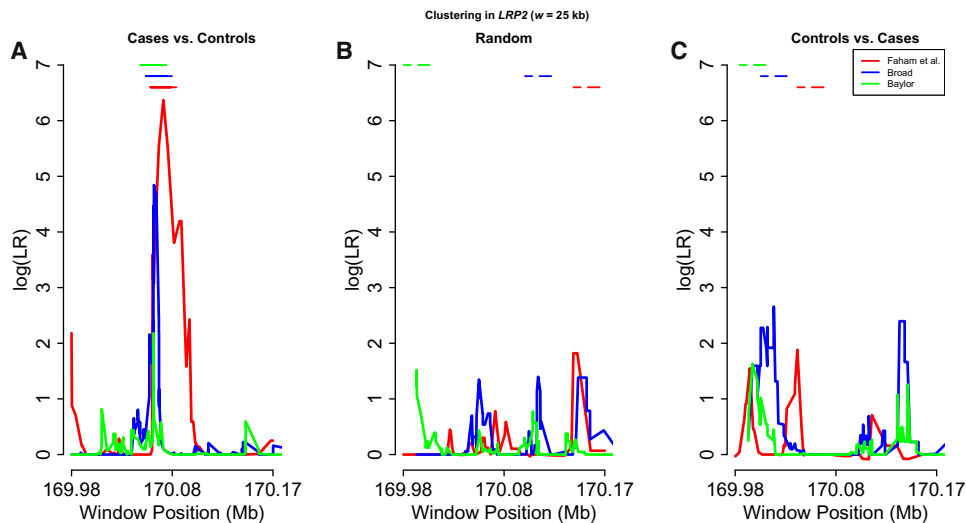


**Figure A1. Clustering of Rare DRVs in *LRP2* for Three Datasets**

(A) Cases versus controls.

(B) Random mix of cases and controls.

(C) Controls versus cases.

Scanning window length is  $w = 25$  kb. The 25 kb windows with maximum LR score are also shown for the three datasets.

mapping reads to hg19. Variants were called with the use of several approaches (including the Genome Analysis Toolkit<sup>45</sup> and Atlas-SNP<sup>46</sup>), and only those variants that passed standard quality-control filters were analyzed.

### Supplemental Data

Supplemental Data include 40 figures and a full list of ARRA Autism Sequencing Consortium authors and affiliations and can be found with this article online at <http://www.cell.com/AJHG>.

### Acknowledgments

The research was partially supported by National Science Foundation grant DMS-1100279 and National Institutes of Health grants R01MH095797 and 1R03HG005908 to I.I.-L. and a Seaver Foundation grant and National Institutes of Health grant MH089025 to J.D.B. The lead investigators for the ARRA Autism Sequencing Consortium are the following: Eric Boerwinkle, Joseph D. Buxbaum, Edwin H. Cook, Jr., Mark J. Daly (communicating principal investigator), Bernie Devlin, Richard Gibbs, Kathryn Roeder, Aniko Sabo, Gerard D. Schellenberg, and James S. Sutcliffe. The full list of investigators is in the [Supplemental Data](#).

Received: January 25, 2012

Revised: February 27, 2012

Accepted: April 19, 2012

Published online: May 10, 2012

### Web Resources

The URLs for data presented herein are as follows:

Online Mendelian Inheritance in Man (OMIM), <http://www.omim.org>

Picard, <http://picard.sourceforge.net/>

PLINK, <http://pngu.mgh.harvard.edu/~purcell/plink/>

### References

- Metzker, M.L. (2010). Sequencing technologies - the next generation. *Nat. Rev. Genet.* *11*, 31–46.
- Li, B., and Leal, S.M. (2008). Methods for detecting associations with rare variants for common diseases: Application to analysis of sequence data. *Am. J. Hum. Genet.* *83*, 311–321.
- Madsen, B.E., and Browning, S.R. (2009). A groupwise association test for rare mutations using a weighted sum statistic. *PLoS Genet.* *5*, e1000384.
- Price, A.L., Kryukov, G.V., de Bakker, P.I., Purcell, S.M., Staples, J., Wei, L.J., and Sunyaev, S.R. (2010). Pooled association tests for rare variants in exon-resequencing studies. *Am. J. Hum. Genet.* *86*, 832–838.
- Liu, D.J., and Leal, S.M. (2010). A novel adaptive method for the analysis of next-generation sequencing data to detect complex trait associations with rare variants due to gene main effects and interactions. *PLoS Genet.* *6*, e1001156.
- King, C.R., Rathouz, P.J., and Nicolae, D.L. (2010). An evolutionary framework for association testing in resequencing studies. *PLoS Genet.* *6*, e1001202.
- Bhatia, G., Bansal, V., Harismendy, O., Schork, N.J., Topol, E.J., Frazer, K., and Bafna, V. (2010). A covering method for detecting genetic associations between rare variants and common phenotypes. *PLoS Comput. Biol.* *6*, e1000954.
- Han, F., and Pan, W. (2010). A data-adaptive sum test for disease association with multiple common or rare variants. *Hum. Hered.* *70*, 42–54.
- Ionita-Laza, I., Buxbaum, J.D., Laird, N.M., and Lange, C. (2011). A new testing strategy to identify rare variants with either risk or protective effect on disease. *PLoS Genet.* *7*, e1001289.
- Neale, B.M., Rivas, M.A., Voight, B.F., Altshuler, D., Devlin, B., Orho-Melander, M., Kathiresan, S., Purcell, S.M., Roeder, K., and Daly, M.J. (2011). Testing for an unusual distribution of rare variants. *PLoS Genet.* *7*, e1001322.

11. Wu, M.C., Lee, S., Cai, T., Li, Y., Boehnke, M., and Lin, X. (2011). Rare-variant association testing for sequencing data with the sequence kernel association test. *Am. J. Hum. Genet.* 89, 82–93.
12. Lin, D.Y., and Tang, Z.Z. (2011). A general framework for detecting disease associations with rare variants in sequencing studies. *Am. J. Hum. Genet.* 89, 354–367.
13. Tzeng, J.Y., Zhang, D., Pongpanich, M., Smith, C., McCarthy, M.I., Sale, M.M., Worrall, B.B., Hsu, F.C., Thomas, D.C., and Sullivan, P.F. (2011). Studying gene and gene-environment effects of uncommon and common variants on continuous traits: a marker-set approach using gene-trait similarity regression. *Am. J. Hum. Genet.* 89, 277–288.
14. Naus, J.I. (1965). The distribution of the size of the maximum cluster of points on a line. *J. Am. Stat. Assoc.* 60, 532–538.
15. Kulldorff, M. (1997). A spatial scan statistic. *Commun Stat Theory Methods.* 26, 1481–1496. Published online June 27, 2007. 10.1080/03610929708831995.
16. Robertson, S.P., Twigg, S.R., Sutherland-Smith, A.J., Biancalana, V., Gorlin, R.J., Horn, D., Kenwick, S.J., Kim, C.A., Morava, E., Newbury-Ecob, R., et al; OPD-spectrum Disorders Clinical Collaborative Group. (2003). Localized mutations in the gene encoding the cytoskeletal protein filamin A cause diverse malformations in humans. *Nat. Genet.* 33, 487–491.
17. Henderson, D.M., Lee, A., and Ervasti, J.M. (2010). Disease-causing missense mutations in actin binding domain 1 of dystrophin induce thermodynamic instability and protein aggregation. *Proc. Natl. Acad. Sci. USA* 107, 9632–9637.
18. Laccione, F., Huppke, P., Hanefeld, F., and Meins, M. (2001). Mutation spectrum in patients with Rett syndrome in the German population: Evidence of hot spot regions. *Hum. Mutat.* 17, 183–190.
19. Bissler, J.J., Cicardi, M., Donaldson, V.H., Gatenby, P.A., Rosen, F.S., Sheffer, A.L., and Davis, A.E., 3rd. (1994). A cluster of mutations within a short triplet repeat in the C1 inhibitor gene. *Proc. Natl. Acad. Sci. USA* 91, 9622–9625.
20. Schneppenheim, R., Michiels, J.J., Obser, T., Oyen, F., Pieconka, A., Schneppenheim, S., Will, K., Zieger, B., and Budde, U. (2010). A cluster of mutations in the D3 domain of von Willebrand factor correlates with a distinct subgroup of von Willebrand disease: type 2A/IIIE. *Blood* 115, 4894–4901.
21. Yue, P., Forrest, W.F., Kaminker, J.S., Lohr, S., Zhang, Z., and Cavet, G. (2010). Inferring the functional effects of mutation through clusters of mutations in homologous proteins. *Hum. Mutat.* 31, 264–271.
22. Frank, R.A., McRae, A.F., Pocklington, A.J., van de Lagemaat, L.N., Navarro, P., Croning, M.D., Komiyama, N.H., Bradley, S.J., Challiss, R.A., Armstrong, J.D., et al. (2011). Clustered coding variants in the glutamate receptor complexes of individuals with schizophrenia and bipolar disorder. *PLoS ONE* 6, e19011.
23. Buxbaum, J.D., Silverman, J.M., Smith, C.J., Kilifarski, M., Reichert, J., Hollander, E., Lawlor, B.A., Fitzgerald, M., Greenberg, D.A., and Davis, K.L. (2001). Evidence for a susceptibility gene for autism on chromosome 2 and for genetic heterogeneity. *Am. J. Hum. Genet.* 68, 1514–1520.
24. Shao, Y., Raiford, K.L., Wolpert, C.M., Cope, H.A., Ravan, S.A., Ashley-Koch, A.A., Abramson, R.K., Wright, H.H., DeLong, R.G., Gilbert, J.R., et al. (2002). Phenotypic homogeneity provides increased support for linkage on chromosome 2 in autistic disorder. *Am. J. Hum. Genet.* 70, 1058–1061.
25. Szatmari, P., Paterson, A.D., Zwaigenbaum, L., Roberts, W., Brian, J., Liu, X.Q., Vincent, J.B., Skaug, J.L., Thompson, A.P., Senman, L., et al; Autism Genome Project Consortium. (2007). Mapping autism risk loci using genetic linkage and chromosomal rearrangements. *Nat. Genet.* 39, 319–328.
26. Wallenstein, S., and Neff, N. (1987). An approximation for the distribution of the scan statistic. *Stat. Med.* 6, 197–207.
27. Davies, R.B. (1977). Hypothesis testing when a nuisance parameter is present only under the alternative. *Biometrika* 64, 247–254.
28. Schaffner, S.F., Foo, C., Gabriel, S., Reich, D., Daly, M.J., and Altshuler, D. (2005). Calibrating a coalescent simulation of human genome sequence variation. *Genome Res.* 15, 1576–1583.
29. Faham, M., Zheng, J., Moorhead, M., Fakhrai-Rad, H., Namsaraev, E., Wong, K., Wang, Z., Chow, S.G., Lee, L., Suyenaga, K., et al. (2005). Multiplexed variation scanning for 1,000 amplicons in hundreds of patients using mismatch repair detection (MRD) on tag arrays. *Proc. Natl. Acad. Sci. USA* 102, 14717–14722.
30. May, P., Woldt, E., Matz, R.L., and Boucher, P. (2007). The LDL receptor-related protein (LRP) family: An old family of proteins with new physiological functions. *Ann. Med.* 39, 219–228.
31. Iossifov, I., Ronemus, M., Levy, D., Wang, Z., Hakker, I., Rosenbaum, J., Yamrom, B., Lee, Y., Narzisi, G., Leotta, A., et al. (2012). De Novo Gene Disruptions in Children on the Autistic Spectrum. *Neuron* 74, 285–299.
32. Kantarci, S., Al-Gazali, L., Hill, R.S., Donnai, D., Black, G.C., Bieth, E., Chassaing, N., Lacombe, D., Devriendt, K., Teebi, A., et al. (2007). Mutations in LRP2, which encodes the multi-ligand receptor megalin, cause Donnai-Barrow and facio-oculo-acoustico-renal syndromes. *Nat. Genet.* 39, 957–959.
33. Zarbalis, K., May, S.R., Shen, Y., Ekker, M., Rubenstein, J.L., and Peterson, A.S. (2004). A focused and efficient genetic screening strategy in the mouse: Identification of mutations that disrupt cortical development. *PLoS Biol.* 2, E219.
34. Willnow, T.E., Armstrong, S.A., Hammer, R.E., and Herz, J. (1995). Functional expression of low density lipoprotein receptor-related protein is controlled by receptor-associated protein in vivo. *Proc. Natl. Acad. Sci. USA* 92, 4537–4541.
35. Spoelgen, R., Hammes, A., Anzenberger, U., Zechner, D., Andersen, O.M., Jerchow, B., and Willnow, T.E. (2005). LRP2/megalyn is required for patterning of the ventral telencephalon. *Development* 132, 405–414.
36. Gajera, C.R., Emich, H., Lioubinski, O., Christ, A., Beckervordersandforth-Bonk, R., Yoshikawa, K., Bachmann, S., Christensen, E.I., Götz, M., Kempermann, G., et al. (2010). LRP2 in ependymal cells regulates BMP signaling in the adult neurogenic niche. *J. Cell Sci.* 123, 1922–1930.
37. Christ, A., Christa, A., Kur, E., Lioubinski, O., Bachmann, S., Willnow, T.E., and Hammes, A. (2012). LRP2 is an auxiliary SHH receptor required to condition the forebrain ventral midline for inductive signals. *Dev. Cell* 22, 268–278.
38. Joshi, P.S., Deshmukh, V., and Golgire, S. (2012). Gorlin-Goltz syndrome. *Dent Res J (Isfahan)* 9, 100–106.
39. Derwińska, K., Smyk, M., Cooper, M.L., Bader, P., Cheung, S.W., and Stankiewicz, P. (2009). PTCH1 duplication in a family with microcephaly and mild developmental delay. *Eur. J. Hum. Genet.* 17, 267–271.
40. Muller, E.A., Aradhya, S., Atkin, J.F., Carmany, E.P., Elliott, A.M., Chudley, A.E., Clark, R.D., Everman, D.B., Garner, S., Hall, B.D., et al. (2012). Microdeletion 9q22.3 syndrome

- includes metopic craniosynostosis, hydrocephalus, macrosomia, and developmental delay. *Am. J. Med. Genet. A.* 158A, 391–399.
41. van der Zwaag, B., Franke, L., Poot, M., Hochstenbach, R., Spierenburg, H.A., Vorstman, J.A., van Daalen, E., de Jonge, M.V., Verbeek, N.E., Brilstra, E.H., et al. (2009). Gene-network analysis identifies susceptibility genes related to glycobiochemistry in autism. *PLoS ONE* 4, e5324.
  42. Franke, L., van Bakel, H., Fokkens, L., de Jong, E.D., Egmont-Petersen, M., and Wijmenga, C. (2006). Reconstruction of a functional human gene network, with an application for prioritizing positional candidate genes. *Am. J. Hum. Genet.* 78, 1011–1025.
  43. DePristo, M.A., Banks, E., Poplin, R., Garimella, K.V., Maguire, J.R., Hartl, C., Philippakis, A.A., del Angel, G., Rivas, M.A., Hanna, M., et al. (2011). A framework for variation discovery and genotyping using next-generation DNA sequencing data. *Nat. Genet.* 43, 491–498.
  44. Li, H., and Durbin, R. (2010). Fast and accurate long-read alignment with Burrows-Wheeler transform. *Bioinformatics* 26, 589–595.
  45. McKenna, A., Hanna, M., Banks, E., Sivachenko, A., Cibulskis, K., Kernytzky, A., Garimella, K., Altshuler, D., Gabriel, S., Daly, M., and DePristo, M.A. (2010). The Genome Analysis Toolkit: A MapReduce framework for analyzing next-generation DNA sequencing data. *Genome Res.* 20, 1297–1303.
  46. Shen, Y., Wan, Z., Coarfa, C., Drabek, R., Chen, L., Ostrowski, E.A., Liu, Y., Weinstock, G.M., Wheeler, D.A., Gibbs, R.A., and Yu, F. (2010). A SNP discovery method to assess variant allele probability from next-generation resequencing data. *Genome Res.* 20, 273–280.